

Magnetic order in the $S=1/2$ two-dimensional molecular antiferromagnet copper pyrazine perchlorate $\text{Cu}(\text{Pz})_2(\text{ClO}_4)_2$

T. Lancaster,* S. J. Blundell, M. L. Brooks, and P. J. Baker

Clarendon Laboratory, Department of Physics, Oxford University, Parks Road, Oxford OX1 3PU, United Kingdom

F. L. Pratt

ISIS Facility, Rutherford Appleton Laboratory, Chilton, Oxfordshire OX11 0QX, United Kingdom

J. L. Manson and M. M. Conner

Department of Chemistry and Biochemistry, Eastern Washington University, Cheney, Washington 99004, USA

F. Xiao and C. P. Landee

Department of Physics, Clark University, Worcester, Massachusetts 01610, USA

F. A. Chaves, S. Soriano,† and M. A. Novak

Instituto de Física, UFRJ, Rio de Janeiro 21945-970, Brazil

T. P. Papageorgiou, A. D. Bianchi,‡ T. Herrmannsdörfer, and J. Wosnitza

Hochfeld-Magnetlabor Dresden (HLD), Forschungszentrum Dresden-Rossendorf, D-01314 Dresden, Germany

J. A. Schlueter

Material Science Division, Argonne National Laboratory, Argonne, Illinois 60439, USA

(Received 12 December 2006; published 21 March 2007)

We present an investigation of magnetic ordering in the two-dimensional $S=1/2$ quantum magnet $\text{Cu}(\text{Pz})_2(\text{ClO}_4)_2$ using specific heat and zero-field muon-spin relaxation ($\mu^+\text{SR}$). The magnetic contribution to the specific heat is consistent with an exchange strength of 17.7(3) K. We find unambiguous evidence for a transition to a state of three-dimensional long-range order below a critical temperature $T_N=4.21(1)$ K using $\mu^+\text{SR}$ even though there is no feature in the specific heat at that temperature. The absence of a specific heat anomaly at T_N is consistent with recent theoretical predictions. The ratio of $T_N/J=0.24$ corresponds to a ratio of intralayer to interlayer exchange constants of $|J'/J|=6.8\times 10^{-4}$, indicative of excellent two-dimensional isolation. The scaled magnetic specific heat of $[\text{Cu}(\text{Pz})_2(\text{HF}_2)]\text{BF}_4$, a compound with an analogous structure, is very similar to that of $\text{Cu}(\text{Pz})_2(\text{ClO}_4)_2$ although both differ slightly from the predicted value for an ideal 2D $S=1/2$ Heisenberg antiferromagnet.

DOI: [10.1103/PhysRevB.75.094421](https://doi.org/10.1103/PhysRevB.75.094421)

PACS number(s): 75.50.Xx, 75.50.Ee, 76.75.+i

I. INTRODUCTION

The properties of systems described by the $S=1/2$ two-dimensional square lattice quantum Heisenberg antiferromagnet (2DSLQHA) model¹ remain one of the most pressing problems in condensed matter physics. The 2DSLQHA model is described by the Hamiltonian

$$H = \sum_{\langle ij \rangle} J \mathbf{S}_i \cdot \mathbf{S}_j, \quad (1)$$

where J is the nearest-neighbor in-plane superexchange interaction. Although long-range magnetic order (LRO) does not occur within the model above zero temperature,² layered materials that are well described by this model inevitably possess some degree of interlayer coupling (quantified by a coupling constant J') that leads to a crossover to a regime of three-dimensional (3D) LRO at a nonzero Néel temperature T_N . The identification of T_N and hence the ratio $k_B T_N/J$ allows the evaluation of the extent to which a material may be described by the 2DSLQHA model.

The measurement of T_N is often problematical in anisotropic spin systems due to the reduced ordered moment that typifies these materials. In addition, the short-range order that exists in the two-dimensional (2D) planes of a layered material above a 3D transition reduces the effective number of degrees of freedom involved in the transition, diminishing the expected anomaly in specific heat.³ Our recent study⁴ of the quasi-one-dimensional (1D) $S=1/2$ chain compound $\text{CuPz}(\text{NO}_3)_2$ [where Pz is pyrazine ($\text{C}_4\text{H}_4\text{N}_2$)] has shown that implanted muons are uniquely sensitive to the presence of magnetic order in quasi-1D materials. In this paper, we present an investigation of the magnetic properties of the two-dimensional analog of $\text{CuPz}(\text{NO}_3)_2$, namely, copper pyrazine perchlorate $[\text{Cu}(\text{Pz})_2(\text{ClO}_4)_2]$. This material has been the subject of several studies aimed at elucidating its properties,^{5–10} although hitherto, no evidence of a magnetic transition has been found. We have carried out detailed specific heat and muon-spin relaxation measurements. The latter provide unambiguous evidence for a transition to a state of 3D LRO. As expected from recent theoretical studies of highly anisotropic spin systems, our specific heat measure-

ments show no anomaly at the critical temperature and are shown to be in very good agreement with the recent predictions of Monte Carlo simulations of the 2DSLQHA.³

Copper pyrazine perchlorate [Cu(Pz)₂(ClO₄)₂] has long been held to be a good example of a 2DSLQHA.⁵ The material is formed from layers consisting of rectangular arrays of Cu²⁺ ions bridged by pyrazine ligands, which provide the intralayer superexchange.¹⁰ The 300 K structure of Cu(Pz)₂(ClO₄)₂ has the Cu²⁺ ions semicoordinated with two disordered, crystallographically inequivalent ClO₄⁻ tetrahedra (one above and one below the layer) with *C2/m* symmetry.⁵ The ClO₄⁻ ions order at low temperatures, where the crystal structure is reduced to *C2/c*, with the two sets of identical pyrazine pairs tilted by 62.8° and 69.1° with respect to the Cu-N coordination plane.¹⁰ This results in a herring-bone configuration rather than in a square lattice. Despite this distortion, magnetic susceptibility measurements fit very well the 2DSLQHA model,^{7,8,10} with $J=17.5$ K and $g=2.11$.

A second copper pyrazine compound, [Cu(Pz)₂(HF₂)]BF₄ has recently been reported.¹¹ X-ray measurements¹¹ show that it has a layered structure similar to that of Cu(Pz)₂(ClO₄)₂, but with adjacent layers bridged by HF₂⁻ ions. The intralayer exchange strength and 3D ordering temperature were found to be 5.7 and 1.54 K, respectively.

II. EXPERIMENTAL DETAILS

A. Specific heat

The heat-capacity measurements on Cu(Pz)₂(ClO₄)₂ have been carried out on four small crystals with a total mass of 75.7 mg fixed on a Cu sample holder containing a Constantan heater and a calibrated Cernox thermometer with Apiezon-N grease. We used a homemade calorimeter attached to a Janis He³ refrigerator, with an automated system based on the semiadiabatic method. The contribution of the sample holder as well as of the grease to the total heat capacity had been subtracted. Specific heat measurements for [Cu(Pz)₂(HF₂)]BF₄ have been reported previously.¹¹

B. Muon-spin relaxation

Zero-field muon-spin relaxation (ZF μ^+ SR) measurements have been made on a powder sample of Cu(Pz)₂(ClO₄)₂ using the MuSR instrument at the ISIS facility, Rutherford Appleton Laboratory, UK. In a μ^+ SR experiment,¹² spin-polarized positive muons are stopped in a target sample, where the muon usually occupies an interstitial position in the crystal. The observed property in the experiment is the time evolution of the muon-spin polarization, the behavior of which depends on the local magnetic field at the muon site. Each muon decays, with an average lifetime of 2.2 μ s, into two neutrinos and a positron, the latter particle being emitted preferentially along the instantaneous direction of the muon spin. Recording the time dependence of the positron emission directions therefore allows the determination of the spin polarization of the ensemble of muons. In our experiments, positrons are detected by detectors placed forward (*F*) and backward (*B*) of the initial muon polarization direction. Histograms $N_F(t)$ and $N_B(t)$ record the number of positrons de-

TABLE I. Fitting coefficients for pure 2DSLQHA specific heat polynomials from Ref. 3.

n	C_n	D_n
1	-0.0036	1.86131
2	0.26197	-11.51455
3	-1.45326	28.45991
4	3.06373	-32.81602
5	-0.38349	18.6304

tected in the two detectors as a function of time following the muon implantation. The quantity of interest is the decay positron asymmetry function, defined as

$$A(t) = \frac{N_F(t) - \alpha_{\text{expt}} N_B(t)}{N_F(t) + \alpha_{\text{expt}} N_B(t)}, \quad (2)$$

where α_{expt} is an experimental calibration constant. $A(t)$ is proportional to the spin polarization of the muon ensemble.

For these measurements, an Oxford Instruments Variox cryostat and a sorption pump cryostat were used,¹³ with a powder sample packed in a silver foil packet (Ag thickness of 25 μ m) and mounted on a silver backing plate. Silver is used since it possesses only a small nuclear moment and so minimizes any background depolarizing signal.

III. RESULTS

A. Specific heat

The magnetic specific heat of the 2DSLQHA has been calculated using a variety of techniques. Early efforts concentrated on high-temperature series expansions,¹⁴ while more recent work has involved quantum Monte Carlo simulations.^{3,15} These studies reveal that the specific heat rises rapidly from zero at low temperature to a rounded maximum (of magnitude 3.8 J/K mol) at a temperature T_{max} of 0.65 J before decreasing at higher temperatures. A rough approximation to the exchange strength is thus $J = T_{\text{max}}/0.65 = 1.54T_{\text{max}}$. The presence of interlayer interactions J' induces a transition to long-range order and causes the existence of a local maximum in the specific heat at T_N ; this maximum is undetectably small for ratios $|J'/J| < 0.01$ but grows rapidly as the ratio approaches unity.³

The magnetic contribution of the ideal 2DSLQHA ($J' = 0$) can be represented as a function of temperature as a ratio of polynomials in powers of T/J using the following equation:

$$C_{\text{mag}} = R \frac{\sum_{n=1}^5 C_n (T/J)^n}{\sum_{n=1}^5 D_n (T/J)^n}, \quad (3)$$

where R is the gas constant and C_n and D_n are the coefficients obtained by fitting data from a Monte Carlo simulation.³ The coefficients appear in Table I. This form is

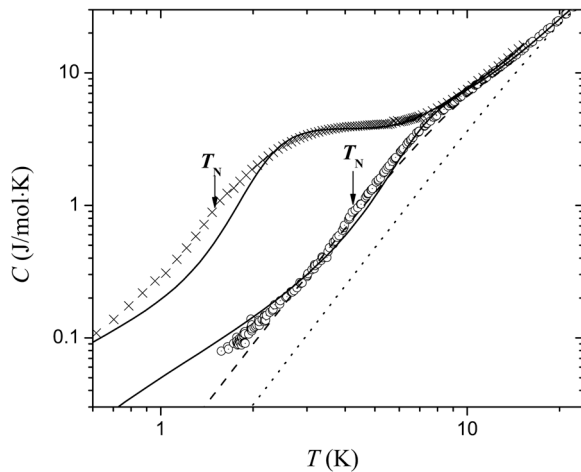


FIG. 1. Specific heats of $\text{Cu}(\text{Pz})_2(\text{ClO}_4)_2$ (\odot) and $[\text{Cu}(\text{Pz})_2(\text{HF}_2)]\text{BF}_4$ (\times) as functions of temperature. The solid lines correspond to the best-fit predictions for the specific heats based on the parameters given in the text. The dashed lines represent the estimated lattice specific heats for $\text{Cu}(\text{Pz})_2(\text{ClO}_4)_2$ (short dashes) and $[\text{Cu}(\text{Pz})_2(\text{HF}_2)]\text{BF}_4$ (long dashes). The arrows mark the temperatures of the magnetic ordering transitions for the two compounds as determined by muon-spin relaxation studies. Note the absence of anomalies in the specific heats at those temperatures.

useful for comparing experimental data to the theoretical predictions and is valid for $T/J > 0.1$.

The molar specific heat data for $\text{Cu}(\text{Pz})_2(\text{ClO}_4)_2$, represented as circles, are shown as a function of temperature in Fig. 1. There is no low-temperature maximum in the data, but an inflection point occurs near 8 K, indicative of a non-lattice contribution. In contrast, the specific heat of the analogous 2D copper pyrazine compound, $[\text{Cu}(\text{Pz})_2(\text{HF}_2)]\text{BF}_4$, also shown in Fig. 1, shows a definite low-temperature anomaly, corresponding to the lower exchange strength of 5.7 K reported for this compound.¹¹ The data sets for both compounds have been analyzed by assuming that the specific heats have both lattice and magnetic contributions. The lattice contribution in the low-temperature region can be approximated as $C_{\text{lattice}} = \alpha T^3 + \beta T^5 + \gamma T^7$, where α , β , and γ are constants to be determined. By modeling the $\text{Cu}(\text{Pz})_2(\text{ClO}_4)_2$ data over the entire range as a sum of the magnetic and lattice contributions, we obtain the best fit for the parameters $J = 17.7(3)$ K, $\alpha = 0.0039(2)$ J/K⁴ mol, $\beta = -2.75 \times 10^{-6}$ J/K⁶ mol, and $\gamma = 6.38 \times 10^{-10}$ J/K⁸ mol, while the corresponding parameters for $[\text{Cu}(\text{Pz})_2(\text{HF}_2)]\text{BF}_4$ are $J = 5.6(1)$ K, $\alpha = 0.0114(5)$ J/K⁴ mol, $\beta = -6(1) \times 10^{-5}$ J/K⁶ mol, and $\gamma = 1.2(2) \times 10^{-7}$ J/K⁸ mol. These values of α correspond to Debye temperatures of 79 (2) and 55 (1) K, respectively. The resultant fits to the two compounds are shown as the solid lines, while the estimated lattice contributions for $\text{Cu}(\text{Pz})_2(\text{ClO}_4)_2$ and $[\text{Cu}(\text{Pz})_2(\text{HF}_2)]\text{BF}_4$ appear as the lines of short dashes and long dashes, respectively. The value of the exchange strength J is in excellent agreement with the value of 17.5 K obtained from the analysis of the magnetic susceptibility data⁷⁻¹⁰ and from the dispersion relation, as obtained by inelastic neutron scattering.¹⁶ Likewise the value of 5.6 K obtained for

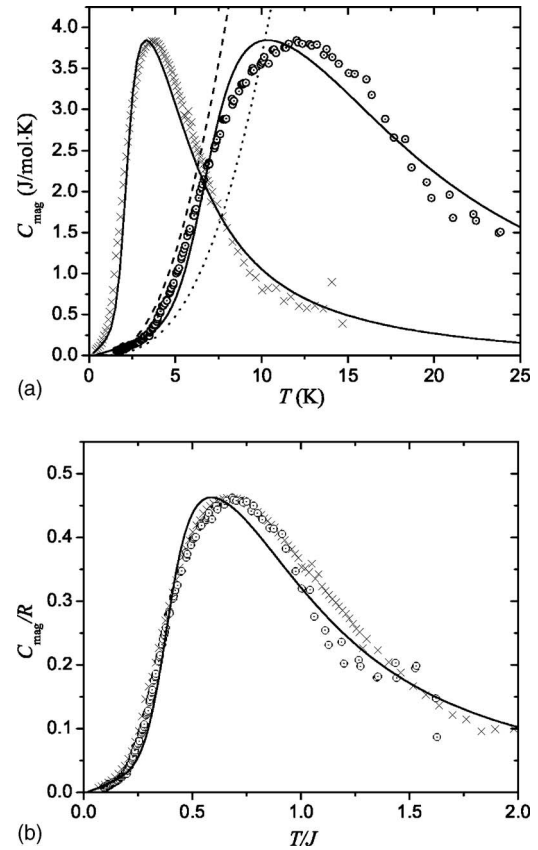


FIG. 2. (a) Magnetic specific heats of $\text{Cu}(\text{Pz})_2(\text{ClO}_4)_2$ (\odot) and $[\text{Cu}(\text{Pz})_2(\text{HF}_2)]\text{BF}_4$ (\times) as functions of temperature with the solid lines corresponding to the best-fit predictions for the magnetic specific heats based on the parameters given in the text. The dashed lines (short dashes for $\text{Cu}(\text{Pz})_2(\text{ClO}_4)_2$ and long dashes for $[\text{Cu}(\text{Pz})_2(\text{HF}_2)]\text{BF}_4$) mark the estimated lattice contributions that were subtracted from the data sets in Fig. 1 to produce the magnetic specific heats. (b) The reduced magnetic specific heats (C_{mag}/R) of $\text{Cu}(\text{Pz})_2(\text{ClO}_4)_2$ (\odot) and $[\text{Cu}(\text{Pz})_2(\text{HF}_2)]\text{BF}_4$ (\times) as functions of the reduced temperature T/J with the solid line corresponding to the theoretical prediction (Ref. 3) for the magnetic specific heat of the 2DSLQHA.

$[\text{Cu}(\text{Pz})_2(\text{HF}_2)]\text{BF}_4$ agrees well with the value of 5.7 K obtained from susceptibility studies.¹¹

The magnetic specific heats, obtained by subtracting estimated lattice contributions from the total specific heats of Fig. 1, are shown in Fig. 2(a), along with the estimated lattice contributions represented by dashed lines, plus the best fit to the theoretical prediction for the 2DSLQHA. While the overall agreement between data and theory is quite good, there are systematic disagreements that are similar for each compound. The theoretical prediction initially rises more slowly at low temperature and surpasses the experimental data while reaching its maximum value at a lower temperature. Nevertheless, the entropy changes for both data sets¹⁷ and the theoretical curve are all within several percent of $R \ln 2$. It is important to note that neither data set shows an anomaly at the temperature of the 3D ordering temperatures {4.21 K for $\text{Cu}(\text{Pz})_2(\text{ClO}_4)_2$ (see below), and 1.54 K for $[\text{Cu}(\text{Pz})_2(\text{HF}_2)]\text{BF}_4$ (see Ref. 11)}, as determined by $\mu^+\text{SR}$.

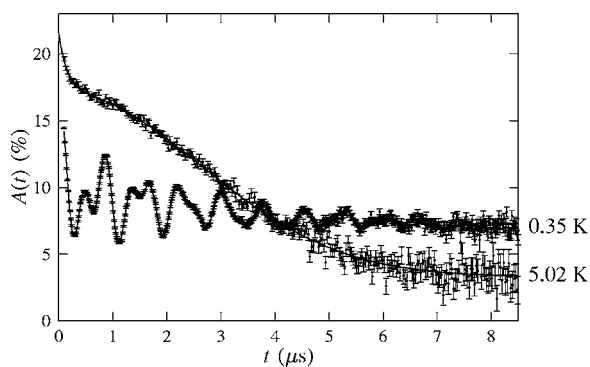


FIG. 3. (a) ZF μ^+ SR spectra in $\text{Cu}(\text{Pz})_2(\text{ClO}_4)_2$ measured at $T=0.35$ K and 5.02 K. At temperatures $T \geq 4.27$ K, Eq. (4) describes the data while the oscillations measured below this temperature are fitted to Eq. (5).

The comparison of experiment and theory is more clearly represented in Fig. 2(b), in which the reduced specific heat (C_{mag}/R) is plotted as a function of the reduced temperature (T/J) for the theory and for both experimental data sets. Here, it is noticed that the two experimental data sets may be superimposed up to $T \approx J$. At higher temperatures, the data for $\text{Cu}(\text{Pz})_2(\text{ClO}_4)_4$ fall below that of $[\text{Cu}(\text{Pz})_2(\text{HF}_2)]\text{BF}_4$ and of the theory. However, by this temperature, the lattice contribution of $\text{Cu}(\text{Pz})_2(\text{ClO}_4)_2$ is more than 90% of the measured value, with commensurate uncertainties in the magnitude of C_{mag} .

B. μ^+ SR

ZF μ^+ SR spectra measured on $\text{Cu}(\text{Pz})_2(\text{ClO}_4)_2$ at two temperatures are shown in Fig. 3. For temperatures $T \geq 4.27$ K, the measured spectra are found to contain two contributions. The first is a fast relaxing component A_1 which dominates the signal at early times and is well described by an exponential function $\exp(-\lambda t)$. The second is a larger, slowly relaxing component A_2 , which dominates at intermediate times and fits to the Kubo Toyabe (KT) function¹⁸ $f_{\text{KT}}(\Delta, t)$, where Δ is the second moment of the static, local magnetic-field distribution defined by $\Delta = \gamma_\mu \sqrt{\langle (B - \langle B \rangle)^2 \rangle}$, where B is the magnitude of the local magnetic field and $\gamma_\mu (= 2\pi \times 135.5 \text{ MHz T}^{-1})$ is the muon gyromagnetic ratio. The KT function is characteristic of spin relaxation due to a random, quasistatic distribution of local magnetic fields at diamagnetic muon sites. We do not observe the recovery in asymmetry at late times that is expected for the static KT function. The lack of this recovery is probably due to slow dynamics in the random field distribution and is crudely modeled here with an exponential term¹⁹ $\exp(-\Lambda_2 t)$. The data were found to be best fitted with the resulting function,

$$A(t) = A_1 \exp(-\Lambda_1 t) + A_2 f_{\text{KT}}(\Delta, t) \exp(-\Lambda_2 t) + A_{\text{bg}} \exp(-\lambda_{\text{bg}} t), \quad (4)$$

where $A_{\text{bg}} \exp(-\lambda_{\text{bg}} t)$ represents a constant background signal from those muons that stop in the sample holder and cryostat tail. The fitting parameters show very little variation

TABLE II. Fitting parameters for Eq. (5) applied to data measured for $T \leq 4.20$ K.

i	A_i (%)	ϕ_i
1	3.127	-39.5
2	2.508	-21.88
3	0.174	96.6
4	2.633	

in the range of $4.27 \leq T \leq 14$ K. The component with amplitude A_1 (found to have relaxation rate $\Lambda_1 \sim 10$ MHz) very likely arises due to the existence of a paramagnetic muon state. In the component with amplitude A_2 , the magnitude of Δ (~ 0.2 MHz) suggests that the random magnetic-field distribution giving rise to the KT function is due to nuclear magnetic moments, implying that the field due to electronic moments at these muon sites is motionally narrowed out of the spectrum due to very rapid fluctuations.

In spectra measured at temperatures $T \leq 4.20$ K, oscillations in the asymmetry spectra are observed at several frequencies (Fig. 3). These oscillations are characteristic of a quasistatic local magnetic field at the muon stopping site, which causes a coherent precession of the spins of those muons with a component of their spin polarization perpendicular to this local field (expected to be 2/3 of the total polarization). The frequency of the oscillations is given by $\nu_i = \gamma_\mu B_i / 2\pi$, where B_i is the magnitude of the local magnetic field at the i th muon site. Any distribution in magnitude of these local fields will result in a relaxation of the oscillating signal, described by relaxation rates¹⁸ λ_i . The presence of oscillations at low temperatures in $\text{Cu}(\text{Pz})_2(\text{ClO}_4)_2$ suggests very strongly that this material is magnetically ordered below 4.20 K.

Three separate frequencies were identified in the low-temperature spectra, corresponding to three magnetically inequivalent muon sites in the material. The precession frequencies, which are proportional to the internal magnetic field as experienced by the muon, are proportional to the magnetic order parameter for these systems. In order to extract the T dependence of the frequencies, the low-temperature data were fitted to the functional form

$$A(t) = A_1 \exp(-\lambda_1 t) \cos(2\pi\nu_1 t + \phi_1) + A_2 \exp(-\lambda_2 t) \cos(2\pi\nu_2 t + \phi_2) + A_3 \exp(-\lambda_3 t) \cos(2\pi\nu_3 t + \phi_3) + A_4 \exp(-\lambda_4 t) + A_{\text{bg}} \exp(-\lambda_{\text{bg}} t), \quad (5)$$

We note that phase offsets ϕ were required to fit the data (see Table II), as observed in our previous μ^+ SR studies of Cu^{2+} systems.^{4,20,21} The amplitudes of the oscillating components were found to be constant in the ordered state and were fixed at the values shown in Table II. These values suggest that the three muon sites have occupation probabilities in the ratio of 0.60:0.33:0.07. The term $A_4 \exp(-\lambda_4 t)$ accounts for the contribution from those muons with a spin component paral-

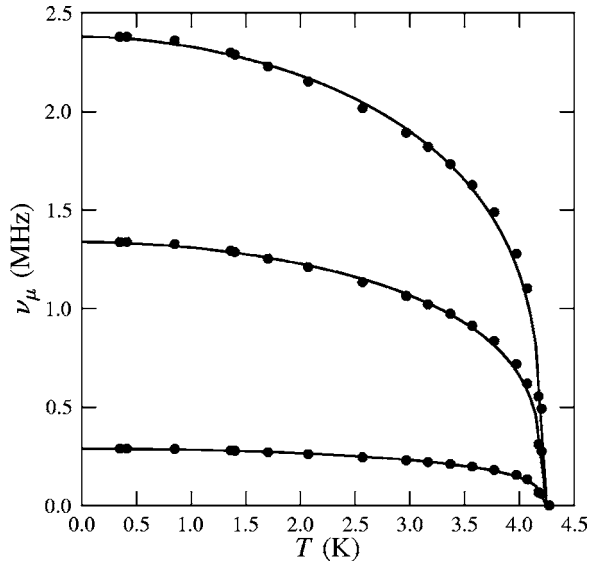


FIG. 4. Temperature evolution of the three magnetic oscillation frequencies in $\text{Cu}(\text{Pz})_2(\text{ClO}_4)_2$, extracted from fits to Eq. (5). The solid lines are fits to the functional form $\nu_i(T) = \nu_i(0)[1 - (T/T_N)^\alpha]^\beta$ (see main text).

lel to the local magnetic field expected to be half of the oscillating amplitude (see above). From Table II, we see that $A_4/(A_1+A_2+A_3) \approx 0.45$ (i.e., the ratio of amplitudes resulting from local magnetic-field components parallel to the initial muon-spin direction to those perpendicular) is close to the expected value of 1/2, suggesting that the material is ordered throughout its bulk. Further evidence for the presence of a magnetic phase transition is provided by the observation that the relaxation rates λ_i tend to increase as T_N is approached from below due to the onset of critical fluctuations.

The three frequencies were found to be in the proportions $\nu_1:\nu_2:\nu_3=1:0.56:0.12$ and were fixed in this ratio in the fitting procedure. The magnitudes of these frequencies were fitted as a function of temperature, with the other parameters in Eq. (5) fixed at the values given in Table II and with the relaxation rates allowed to vary. The resulting temperature evolution of the precession frequencies is shown in Fig. 4. From the fits of the data to the form $\nu_i(T) = \nu_i(0)[1 - (T/T_N)^\alpha]^\beta$, we estimate $T_N=4.21(1)$ K, $\alpha=1.8(3)$, $\beta=0.29(2)$, $\nu_1(0)=2.38(3)$ MHz, $\nu_2(0)=1.33(2)$ MHz, and $\nu_3(0)=0.29(2)$ MHz.

IV. DISCUSSION

A method for estimating the interlayer coupling constant J' in 3D arrays of 2DSLQHA has recently been developed based on a modified random phase approximation, modeled with classical and quantum Monte Carlo simulations.²² This approach leads to an empirical formula relating J' and T_N ,

$$|J'/J| = \exp\left(b - \frac{4\pi\rho_s}{T_N}\right), \quad (6)$$

where ρ_s is the spin stiffness given²³ by $\rho_s=0.183J$ and $b=2.43$ for $S=1/2$. Using $J=17.7$ K, we obtain $\rho_s=3.26$ K

TABLE III. Parameters for the layered compounds $\text{Sr}_2\text{CuO}_2\text{Cl}_2$ (Ref. 24), $\text{Cu}(\text{Pz})_2(\text{ClO}_4)_2$, $[\text{Cu}(\text{Pz})_2(\text{HF}_2)]\text{BF}_4$ (Ref. 11), $\text{Ca}_{0.85}\text{Sr}_{0.15}\text{CuO}_2$ (Ref. 25), and $(5\text{MAP})_2\text{CuBr}_4$ (Ref. 26) with values of $|J'/J|$ estimated from Eq. (6).

	$ J /k_B$ (K)	T_N (K)	$ k_B T_N/J $	$ J'/J $
$\text{Sr}_2\text{CuO}_2\text{Cl}_2$	1451	256.5	0.18	2.5×10^{-5}
$\text{Cu}(\text{Pz})_2(\text{ClO}_4)_2$	17.7	4.21	0.24	6.8×10^{-4}
$[\text{Cu}(\text{Pz})_2(\text{HF}_2)]\text{BF}_4$	5.7	1.54	0.27	2.3×10^{-3}
$\text{Ca}_{0.85}\text{Sr}_{0.15}\text{CuO}_2$	1535	537	0.35	1.6×10^{-2}
$(5\text{MAP})_2\text{CuBr}_4$	6.5	3.8	0.58	2.1×10^{-1}

and $|J'/J|=6.8 \times 10^{-4}$. Table III compares these parameters to those for other 2D layered compounds. We see that $\text{Cu}(\text{Pz})_2(\text{ClO}_4)_2$ compares very favorably as a highly anisotropic system, with the layers around an order of magnitude better isolated than those in $\text{Ca}_{0.85}\text{Sr}_{0.15}\text{CuO}_2$, although not as successful a realization of a 2DSLQHA as $\text{Sr}_2\text{CuO}_2\text{Cl}_2$, where Eq. (6) yields $|J'/J| \sim 10^{-5}$. The J'/J ratios were obtained assuming perfect Heisenberg exchange interactions. The presence of any exchange anisotropy will also raise the ratio T_N/J . So, by ignoring the anisotropy fields while using Eq. (6), we are setting an upper bound for the J'/J ratios.

$\text{Cu}(\text{Pz})_2(\text{ClO}_4)_2$ and $[\text{Cu}(\text{Pz})_2(\text{HF}_2)]\text{BF}_4$ contain structurally similar copper pyrazine layers separated either by the bulky perchlorate groups or by the HF_2 anions. Their intralayer exchange strengths differ by a factor of 3 (17.7 and 5.6 K), but their low ratios of T_N/J show them to be well isolated ($J'/J \sim 10^{-3}$, see Table III). As seen in Fig. 2(b), their magnetic specific heats are essentially identical up to relative temperatures of $T \approx J$. Nevertheless, there is noticeable difference between their behavior and that predicted for isolated 2DSLQHA model systems.³ This difference may arise from the small terms in the Hamiltonian relevant for the compounds but ignored in the Monte Carlo simulation. Studies of $\text{Cu}(\text{Pz})_2(\text{ClO}_4)_2$ in the magnetically ordered state show the presence of about a 0.4 T anisotropy field.²⁷ While small compared to the 60 T exchange field, this anisotropy field will break the rotational symmetry of the Heisenberg Hamiltonian and will modify the low-temperature behavior. It will be necessary to examine the specific heat of the quasi-2DSLQHA in the presence of both weak interlayer interactions as well as weak anisotropies to understand these effects qualitatively.

V. CONCLUSION

We have examined the 2D Heisenberg antiferromagnet $\text{Cu}(\text{Pz})_2(\text{ClO}_4)_2$ using specific heat and $\mu^+\text{SR}$ techniques. The value of the exchange strength obtained [$J=17.7(3)$ K] from the magnetic specific heat is in excellent agreement with values obtained from susceptibility⁷⁻¹⁰ and neutron scattering¹⁶ experiments. The muon-spin relaxation studies demonstrate the existence of 3D long-range magnetic order throughout the bulk of the sample in $\text{Cu}(\text{Pz})_2(\text{ClO}_4)_2$ at temperatures below $T_N=4.21(1)$ K. The value of T_N/J (0.24)

corresponds to a very low ratio of interlayer to intralayer exchange strengths ($|J'/J|=6.8 \times 10^{-4}$). The combination of good isolation of the magnetic layers plus relatively small exchange strength makes $\text{Cu}(\text{Pz})_2(\text{ClO}_4)_2$, as well as $[\text{Cu}(\text{Pz})_2(\text{HF}_2)]\text{BF}_4$, good candidates for studies of the field dependence of the energy spectrum of the 2DSLQHA.^{28,29}

The magnetic ordering transition is readily apparent in the $\mu^+\text{SR}$ data (Fig. 3) even though no anomaly is apparent in the specific heat results at that temperature for $[\text{Cu}(\text{Pz})_2(\text{HF}_2)]\text{BF}_4$ [Fig. 2(a)]. The absence of an ordering peak in the specific heat for well isolated low-dimensional magnets was previously anticipated³ in Monte Carlo studies. These demonstrate that most of the available spin entropy ($R \ln 2$ per mole) is associated with the development of in-plane correlations which give rise to the broad peak in C_{mag} centered around $T=0.65J$. This leaves little remaining entropy to be associated with the 3D ordering at $T=T_N$. The critical temperature of $\text{Cu}(\text{Pz})_2(\text{ClO}_4)_2$ was also not detected by previous inelastic neutron-scattering experiments on poly-

crystalline samples; only after adequate single crystals became available could the transition be observed with this technique.¹⁶ These results emphasize the value of muons in detecting magnetic order in polycrystalline materials.

ACKNOWLEDGMENTS

The authors are grateful to Philip King at ISIS for technical assistance. This work is supported by the EPSRC (UK) and by an award from Research Corporation (USA). T.L. acknowledges support from the 1851 Commission (UK). F.A.C., S.S., and M.A.N. are grateful for the financial support from CNPq, CAPES, and FAPERJ (Brazil). Work at Argonne National Laboratory was supported by the Office of Basic Energy Sciences, Division of Materials Science, U.S. Department of Energy under Contract No. DE-AC02-06CH11357. The authors thank Pinaki Sengupta for the use of his QMC simulation results.

*Electronic address: t.lancaster1@physics.ox.ac.uk

†Present address: DIRO-UFF, Rio das Ostras, Rio de Janeiro, Brazil.

‡Present address: Department of Physics and Astronomy, University of California, Irvine, CA 92697, USA.

¹E. Manousakis, *Rev. Mod. Phys.* **53**, 1 (1991); M. A. Kastner, R. J. Birgeneau, G. Shirane, and Y. Endoh, *ibid.* **70**, 897 (1998).

²N. D. Mermin and H. Wagner, *Phys. Rev. Lett.* **17**, 1133 (1966).

³P. Sengupta, A. W. Sandvik, and R. R. P. Singh, *Phys. Rev. B* **68**, 094423 (2003).

⁴T. Lancaster, S. J. Blundell, M. L. Brooks, P. J. Baker, F. L. Pratt, J. L. Manson, C. P. Landee, and C. Baines, *Phys. Rev. B* **73**, 020410(R) (2006).

⁵J. Darriet, M. S. Hassad, E. N. Duesler, and D. N. Hendrickson, *Inorg. Chem.* **18**, 2679 (1979).

⁶M. S. Haddad, D. N. Hendrickson, J. P. Cannady, R. S. Drago, and D. S. Bieksza, *J. Am. Chem. Soc.* **101**, 898 (1979).

⁷M. M. Turnbull, A. S. Albrecht, G. B. Jameson, and C. P. Landee, *Mol. Cryst. Liq. Cryst. Sci. Technol., Sect. A* **334**, 957 (1999).

⁸A. S. Albrecht, C. P. Landee, Z. Slanic, and M. M. Turnbull, *Mol. Cryst. Liq. Cryst. Sci. Technol., Sect. A* **305**, 333 (1997).

⁹J. Choi, J. D. Woodward, J. L. Musfeldt, C. P. Landee, and M. M. Turnbull, *Chem. Mater.* **15**, 2979 (2003).

¹⁰F. M. Woodward, P. J. Gibson, G. Jameson, C. P. Landee, M. M. Turnbull, and R. D. Willet, *Inorg. Chem.* (to be published).

¹¹J. L. Manson, M. M. Conner, J. A. Schlueter, T. Lancaster, S. J. Blundell, M. L. Brooks, F. Pratt, T. Papageorgiou, A. D. Bianchi, J. Wosnitza, and M. Whangbo, *Chem. Commun. (Cambridge)* **2006**, 4894 (2006).

¹²S. J. Blundell, *Contemp. Phys.* **40**, 175 (1999).

¹³<http://www.isis.rl.ac.uk/muons/musr/index.htm>

¹⁴R. Navarro, in *Magnetic Properties of Layered Transition Metal Compounds*, edited by L. J. de Jongh (Kluwer Academic, Dordrecht, 1990).

¹⁵M. S. Makivic and H. Q. Ding, *Phys. Rev. B* **43**, 3562 (1991).

¹⁶M. Kenzelmann (unpublished).

¹⁷The magnetic specific heat data for $[\text{Cu}(\text{Pz})_2(\text{HF}_2)](\text{BF}_4)$ in Fig. 2 was multiplied by 12% to match the theoretical amplitude for C_{mag} of the 2DSLQHA. If this 12% change is not included, there is then a discrepancy between the theoretical prediction and the measured data which may be due to a shift of the entropy towards lower temperatures, where the 3D ordering occurs. The fit described in the main text cannot, in fact, take account of this ordering. If the unmultiplied data are fit to a combination of magnetic and lattice contributions, a good fit is obtained with parameters $J/k=5.8 \text{ K}$, $\alpha=0.00861 \text{ J/mol K}^4$, $\beta=-2.6448 \times 10^{-5} \text{ J/mol K}^6$, and $\gamma=3.642 \times 10^{-8} \text{ J/mol K}^8$. For either fit, the magnetic entropy of $R \ln 2$ is obtained within several percent.

¹⁸R. S. Hayano, Y. J. Uemura, J. Imazato, N. Nishida, T. Yamazaki, and R. Kubo, *Phys. Rev. B* **20**, 850 (1979).

¹⁹F. L. Pratt, S. J. Blundell, T. Lancaster, C. Baines, and S. Takagi, *Phys. Rev. Lett.* **96**, 247203 (2006).

²⁰T. Lancaster, S. J. Blundell, F. L. Pratt, M. L. Brooks, J. L. Manson, E. K. Brechin, C. Cadiou, D. Low, E. J. L. McInnes, and R. E. P. Winpenny, *J. Phys.: Condens. Matter* **16**, S4563 (2004).

²¹J. L. Manson, T. Lancaster, L. C. Chapon, S. J. Blundell, J. A. Schlueter, M. L. Brooks, F. L. Pratt, C. L. Nygren, and J. S. Qualls, *Inorg. Chem.* **44**, 989 (2005).

²²C. Yasuda, S. Todo, K. Hukushima, F. Alet, M. Keller, M. Troyer, and H. Takayama, *Phys. Rev. Lett.* **94**, 217201 (2005).

²³B. B. Beard, R. J. Birgeneau, M. Greven, and U.-J. Wiese, *Phys. Rev. Lett.* **80**, 1742 (1998).

²⁴M. Greven, R. J. Birgeneau, Y. Endoh, M. A. Kastner, B. Keimer, M. Matsuda, G. Shirane, and T. R. Thurston, *Phys. Rev. Lett.* **72**, 1096 (1994).

²⁵T. Siegrist, S. M. Zahurak, D. W. Murphy, and R. S. Roth, *Nature (London)* **334**, 231 (1998); D. Vaknin, E. Caignol, P. K. Davies, J. E. Fischer, D. C. Johnston, and D. P. Goshorn, *Phys. Rev. B* **39**, 9122 (1989); Y. Tokura, S. Koshihara, T. Arima, H. Takagi,

- S. Ishibashi, T. Ido, and S. Uchida, Phys. Rev. B **41**, 11657 (1990).
- ²⁶F. M. Woodward, A. S. Albrecht, C. M. Wynn, C. P. Landee, and M. M. Turnbull, Phys. Rev. B **65**, 144412 (2002).
- ²⁷F. Xiao, C. P. Landee *et al.* (unpublished).
- ²⁸O. F. Syljuåsen and P. A. Lee, Phys. Rev. Lett. **88**, 207207 (2002).
- ²⁹M. E. Zhitomirsky and A. L. Chernyshev, Phys. Rev. Lett. **82**, 4536 (1999).